Ligand Design

International Edition: DOI: 10.1002/anie.201713304
German Edition: DOI: 10.1002/ange.201713304

Design, Synthesis, and Application of Chiral C_2-Symmetric Spiroketal-Containing Ligands in Transition-Metal Catalysis

*Alonso J. Argüelles, Siyuan Sun, Brenna G. Budaitis, and Pavel Nagorny**

Abstract: *We present an expedient and economical route to a new spiroketal-based C_2-symmetric chiral scaffold, termed SPIROL. Based on this spirocyclic scaffold, several chiral ligands were generated. These ligands were successfully employed in an array of stereoselective transformations, including in iridium-catalyzed hydroarylations (up to 95% ee), palladium-catalyzed allylic alkylations (up to 97% ee), intermolecular palladium-catalyzed Heck couplings (up to 94% ee), and rhodium-catalyzed dehydroalanine hydrogenation (up to 93% ee).*

Asymmetric transition-metal catalysis is one of the most practical and powerful approaches to achieve stereocontrol.[1] Its successful application heavily relies on both the powerful and enabling chemistry of transition metals and the versatility of chiral organic ligands to enable stereoselective transformations. The generality and utility of this mode of activation stress the need for a wide variety of structurally diverse chiral ligands to be able to fine-tune the stereocontrol in these reactions. Since the popularization of (1,1′-binaphthalene)-2,2′-diylbis(diphenylphosphine) (BINAP), chiral phosphine ligands have dominated the field of asymmetric transition-metal catalysis,[2,3] and organic chemists have strived to provide alternative chiral backbones with superior performance in catalysis.[4] SPINOL-derived ligands, such as 7,7′-bis(diarylphosphino)-2,2′,3,3′-tetrahydro-1,1′-spirobiindenes (SDPs),[5] have been used with great success in the past decades (Figure 1 A, left).[6] Although their performance is notable, high prices and tedious preparation methods pose severe limitations to the application of these ligands. Recent efforts of Tan and co-workers focused on addressing some of these problems by developing an optimized synthesis of SPINOL.[7] However, this approach still suffers from the obligatory use of SPINOL-derived phosphoric acids, which are expensive and commercially unavailable on a large scale.

Based on our prior work on the asymmetric formation of axially chiral spiroketals,[8] we propose a new, easily accessible, spiroketal-based C_2-symmetric chiral scaffold termed SPIROL (Figure 1 A, right). Whereas spiroketal moieties tend to be labile under strongly acidic conditions, the majority of transition-metal-catalyzed reactions are not carried out under highly acidic conditions. For these reasons as well as their high accessibility, acetal-[9] and spiroketal-containing[10] ligands have proven to be of great value in asymmetric catalysis (Figure 1 B). We surmised that the introduction of bulky 7,7′-substituents such as PPh_2 would render both axially pseudoenantiomeric diastereomers kinetically stable under a variety of conditions (Figure 1 C). Moreover, the additional stereocenters at the benzylic 3,3′-positions would prevent epimerization of the more stable *S*,*S*,*S* diastereomer ($\Delta G° = 2.3$ kcal mol^{-1} for SPIRAP) even under equilibrating conditions. This work describes the development of a reliable dimerizative condensation that provides rapid access to chiral SPIROL on large scale, and the application of SPIROL-based ligands in various Pd-, Ir-, and Rh-catalyzed enantioselective transformations. These results, along with computational studies, suggest that the *S*,*S*,*S* diastereomers are structurally and electronically similar to SPINOL-based ligands, whereas the axially pseudoenantiomeric *R*,*S*,*S* diastereomers represent a structurally different scaffold. We believe that these features, in combination with the ease of preparation and higher level of tunability, render SPIROL ligands of great value to asymmetric catalysis.

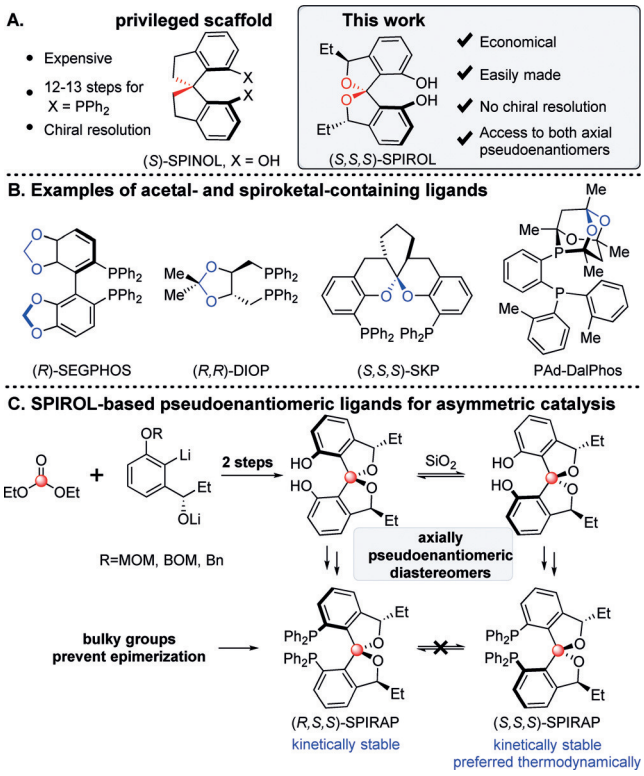

Figure 1. A) Privileged SPINOL scaffold (left) and our proposed scaffold (right). B) Acetal- and spiroketal-containing commercially available phosphine ligands. C) Pseudoenantiomeric SPIROL-based ligands.

[*] A. J. Argüelles, S. Sun, B. G. Budaitis, Prof. Dr. P. Nagorny
Department of Chemistry, University of Michigan
Ann Arbor, MI 48109 (USA)
E-mail: nagorny@umich.edu

Supporting information and the ORCID identification number(s) for the author(s) of this article can be found under: https://doi.org/10.1002/anie.201713304.

We commenced our studies by investigating the highly enantioselective alkylation of protected 3-hydroxybenzaldehyde **1** (Scheme 1). While commercially available *N*,*N*-dibutylnorephedrine (DBNE) catalyzes highly enantioselective additions to different protected aldehydes (R = MOM, BOM, Bn),[11] readily available aziridine-based organocatalysts can also be used to attain the desired products **2** in practically enantiopure form (see the Supporting Information).[12] Treatment of the resulting alcohol **2** with two equivalents of *n*-butyllithium in toluene afforded the dilithiated species **3** in a regioselective fashion (see the Supporting Information), which was then captured by diethyl carbonate to produce the desired spiroketal **6** in good yields and excellent diastereoselectivity. This transformation is proposed to proceed through the intermediacy of isobenzofuranone **4** and then adduct **5**, which subsequently collapses to **6** upon treatment with acetic acid. This unprecedented dimerization can be carried out on decagram scale and provides a quick means for accessing protected SPIROL.

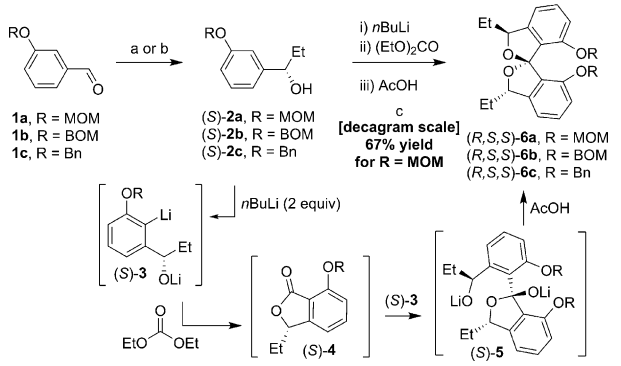

Scheme 1. Highly diastereoselective spiroketalization of benzylic alcohols **2**. Reagents and conditions: a) For R = Bn/MOM: (−)-DBNE (7 mol%), Et_2Zn (1 M in hexanes, 2.2 equiv), hexanes, 0 °C; 97% yield, 94% *ee* (R = MOM); 82% yield, 91% *ee* (R = Bn); b) for R = Bn/BOM/MOM: aziridine diphenyl((*S*)-1-((*S*)-1-phenylethyl)aziridin-2-yl)methanol (5 mol%), Et_2Zn (1 M in hexanes, 2.2 equiv), toluene, 0 °C; 97% yield, >99% *ee* (R = MOM); 91% yield, 99% *ee* (R = BOM); 99% yield, 98% *ee* (R = Bn); the *R*,*S* aziridine organocatalyst could be used to obtain (*R*)-**2** in excellent *ee* (see the Supporting Information); c) i) *n*BuLi (1 M in hexanes, 2.0 equiv), toluene, 0 °C to RT; ii) diethyl carbonate (0.55 equiv), RT; iii) AcOH (excess), RT; 67% yield (79% based on recovered starting material (BRSM)), >20:1 d.r. (R = MOM); 59% yield (64% BRSM), >20:1 d.r. (R = BOM); 42% yield (66% BRSM), >20:1 d.r. (R = Bn). BOM = benzyloxymethyl, MOM = methoxymethyl.

Computational studies[13] showed that the pseudoenantiomeric diol diastereomers (*R*,*S*,*S*)-**7** and (*S*,*S*,*S*)-**7** have near-equal gas-phase energies (1.0 kcal mol^{-1} difference favoring (*S*,*S*,*S*)-**7**), and we therefore surmised that we would be able to equilibrate them under mildly acidic conditions to obtain mainly (*S*,*S*,*S*)-**7**, or suppress the epimerization to favor (*R*,*S*,*S*)-**7**. To our delight, deprotection of substrates **6a**–**6c** proceeded with excellent yields and moderate selectivities for either diastereomer of SPIROL scaffold **7** (1:3.8 d.r. favoring (*R*,*S*,*S*)-**7** to 1.9:1 favoring (*S*,*S*,*S*)-**7**; Scheme 2 and the Supporting Information). During the acidic deprotection of

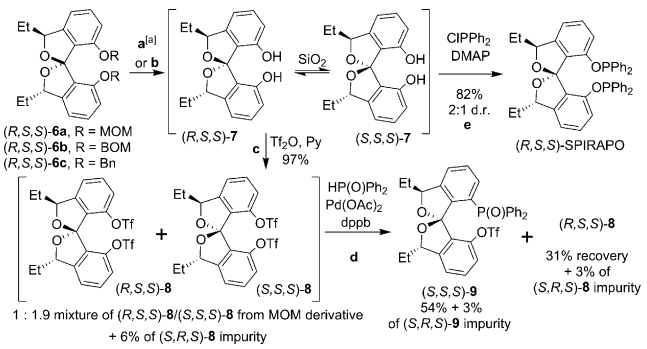

Scheme 2. Diol equilibration and chemical separation of diastereomers. Reagents and conditions: a) AcCl (2 equiv), MeOH, 0 °C to RT; 91% yield, 3.8:1 or 1:1.9 d.r. depending on the conditions and 6% (*S*,*R*,*S*)-**8** impurity (R = MOM); 87% yield, 1:1.3 d.r. and 10% (*S*,*R*,*S*)-**8** impurity (R = BOM); b) for R = Bn: H_2 (balloon), $NaHCO_3$ (9 equiv), MeOH, RT; 94% yield, 1:6.9 d.r.; c) Tf_2O (2.4 equiv), pyridine (5.3 equiv), DCM, 0 °C to RT; 97% yield, with conserved d.r.; d) HP(O)Ph_2 (0.9 equiv), Pd(OAc)$_2$ (4.1 mol%), dppb (4.1 mol%), DIPEA (2.3 equiv), DMSO, 80 °C; for a 1:1.9 d.r. mixture with 6% (*S*,*R*,*S*)-**8** impurity: 54% yield of (*S*,*S*,*S*)-**9**, with 3% of (*S*,*R*,*S*)-**9**, and 31% recovery of (*R*,*S*,*S*)-**8** with 3% (*S*,*R*,*S*)-**8** impurity; e) $PPPh_2Cl$ (2.5 equiv), DMAP (0.1 equiv), NEt_3 (4 equiv), DCM, 82% yield over 2 steps, 2:1 d.r. favoring (*R*,*S*,*S*)-SPIRAPO. [a] (*R*,*S*,*S*)-**7** is the major diastereomer that is initially formed; however, prolonged exposure to acids, including SiO_2, results in epimerization to give (*S*,*S*,*S*)-**7** as the major diastereomer (see the Supporting Information for details). DIPEA = *N*,*N*-diisopropylethylamine, DMAP = 4-dimethylaminopyridine, dppb = 1,4-bis(diphenylphosphino)butane, Py = pyridine, Tf = trifluoromethanesulfonyl.

(*R*,*S*,*S*)-**6a** or (*R*,*S*,*S*)-**6b**, a small amount of the undesired (*S*,*R*,*S*)-**7** diol was also formed (ca. 6% for R = MOM). The diastereomers were not separated at this stage as they were not configurationally stable, and their mixture was converted into the corresponding configurationally stable ditriflates (*R*,*S*,*S*)-**8** and (*S*,*S*,*S*)-**8**.

Despite their similar R_f values, the ditriflates could be separated by conventional chromatographic techniques. However, we also identified a method that is more convenient for large-scale purification and takes advantage of the different reactivities of these species. The mixture of ditriflates was subjected to a palladium-catalyzed coupling with diphenylphosphine oxide at 80 °C. We observed that at this temperature, the (*S*,*S*,*S*)-**8** diastereomer reacted in excellent yield to give (*S*,*S*,*S*)-**9** while the (*R*,*S*,*S*)-**8** diastereomer was recovered almost quantitatively. The (*S*,*R*,*S*)-**8** impurity reacted partially but was easily removed by recrystallization from cyclohexane.

Afterwards, the triflate-substituted phosphine oxide (*S*,*S*,*S*)-**9** was transformed into the respective diphosphine. Reduction with trichlorosilane afforded triflate-substituted phosphine (*S*,*S*,*S*)-**10**, which was then subjected to a second coupling with diphenylphosphine oxide to generate phosphine-substituted phosphine oxide (*S*,*S*,*S*)-SPIRAP(O), the structure of which was confirmed by X-ray crystallography. In addition, direct coupling of phosphine triflate (*S*,*S*,*S*)-**10** with diphenylphosphine provided (*S*,*S*,*S*)-SPIRAP in excellent yields (Scheme 3).

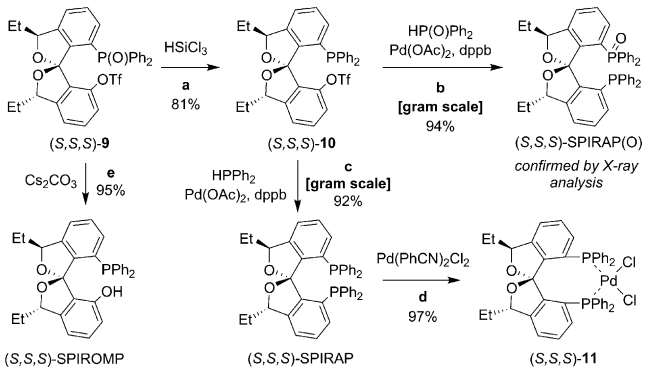

Scheme 3. Functionalization of scaffold **9** into various ligands. Reagents and conditions: a) $HSiCl_3$ (16 equiv), DIPEA (40 equiv), toluene, 80 °C, 81 % yield; b) $HP(O)Ph_2$ (2 equiv), DIPEA (5 equiv), $Pd(OAc)_2$ (5 mol %), dppb (5 mol %), DMSO, 100 °C, 94 % yield; c) $HPPh_2$ (3 equiv), DIPEA (6.1 equiv), $Pd(OAc)_2$ (10 mol %), dppb (11 mol %), DMF, 100 °C, 92 % yield; d) $Pd(PhCN)_2Cl_2$ (1.0 equiv), benzene, 97 % yield; e) Cs_2CO_3 (5 equiv), DMF, 80 °C, 95 %.

In line with the aforementioned studies, the recovered ditriflate (*R*,*S*,*S*)-**8** was recrystallized from cyclohexane and reacted in good yields with diphenylphosphine oxide under similar coupling conditions, albeit at 100 °C, to provide pure (*R*,*S*,*S*)-**9**, which was likewise elaborated to (*R*,*S*,*S*)-SPIRAP-(O) and (*R*,*S*,*S*)-SPIRAP in good yields. The absolute stereochemistry of (*S*,*R*,*R*)-SPIRAP(O) obtained by an identical route using (*R*)-**2a** was confirmed by X-ray crystallography (see the Supporting Information). All of the intermediates towards (*R*,*S*,*S*)-SPIRAP were found to be configurationally stable, which led us to believe that epimerization is mostly impeded for steric reasons. In addition, other ligands such as diphosphinite (*R*,*S*,*S*)-SPIRAPO (Scheme 2) and catalysts such as (*S*,*S*,*S*)-SPIROMP as well $PdCl_2$ complexes **11** (Scheme 3) were conveniently generated. The SPIRAPO was obtained as a 2:1 mixture of the *R*,*S*,*S* and *S*,*S*,*S* diastereomers (82 % yield), which is reflective of the d.r. of the initially used mixture of isomers **7**, and could be separated by chromatography.

The ligands synthesized above were then tested in various reported asymmetric catalysis applications (Scheme 4). We were pleased to find that (*S*,*S*,*S*)-SPIRAP is an exceptional ligand in the iridium-catalyzed hydroarylation of methylated cinnamyl alcohol **12** and 2-phenylpyridine (**13**), which provided better enantiocontrol (entry 5) than the BINAP- (entries 1 and 3) and SEGPHOS-based (entry 2) ligands recently explored by Nishimura and co-workers (Scheme 4 A).[14] Interestingly, its diastereomer, (*R*,*S*,*S*)-SPIRAP, was not a viable ligand for this reaction, and no product was detected (entry 6). Similarly, (*S*,*S*,*S*)-SPIRAP performed very well in the palladium-catalyzed allylic alkylation of chalcone derivative **15** with dimethyl malonate **16** to afford chiral diester **17** in 94 % yield and 97 % *ee* (Scheme 4 B, entry 8), which is comparable to the results obtained with commercial (*S*)-SDP (entry 7).[15] Remarkably, the pseudoenantiomeric ligand (*R*,*S*,*S*)-SPIRAP favored the other enantiomer of the product in 88 % *ee* (entry 9). The phosphine oxide/phosphine ligand (*S*,*S*,*S*)-SPIRAP(O) was also used with great success in a palladium-catalyzed Heck reaction of 2-vinylphenyl triflate

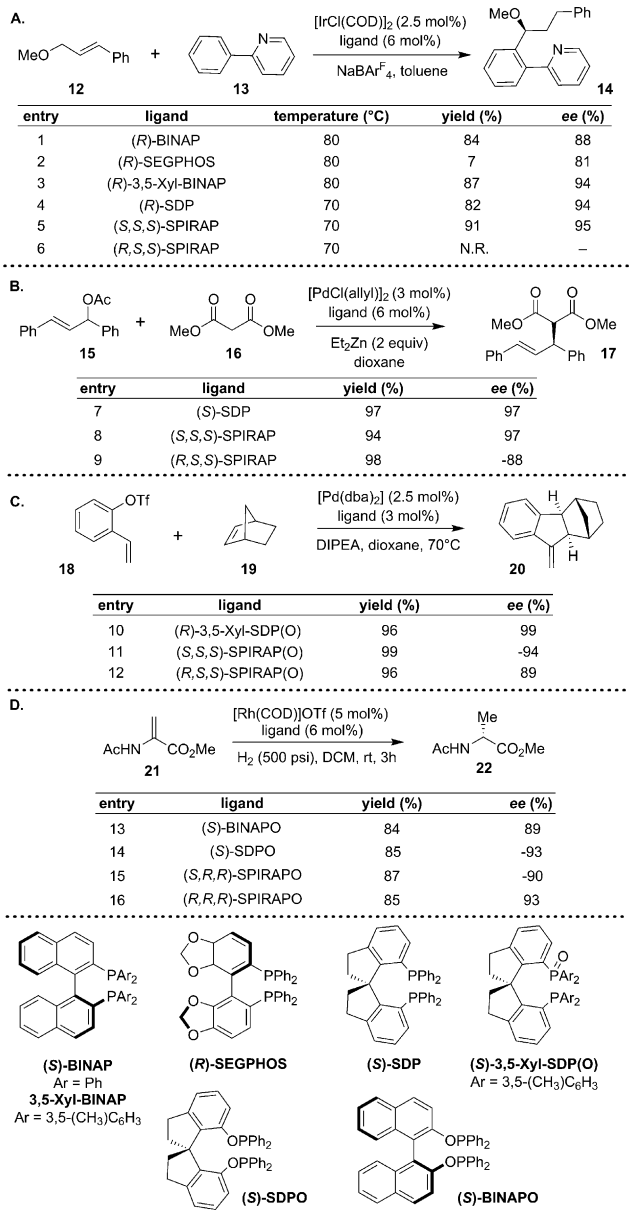

entry	ligand	temperature (°C)	yield (%)	*ee* (%)
1	(*R*)-BINAP	80	84	88
2	(*R*)-SEGPHOS	80	7	81
3	(*R*)-3,5-Xyl-BINAP	80	87	94
4	(*R*)-SDP	70	82	94
5	(*S*,*S*,*S*)-SPIRAP	70	91	95
6	(*R*,*S*,*S*)-SPIRAP	70	N.R.	–

entry	ligand	yield (%)	*ee* (%)
7	(*S*)-SDP	97	97
8	(*S*,*S*,*S*)-SPIRAP	94	97
9	(*R*,*S*,*S*)-SPIRAP	98	-88

entry	ligand	yield (%)	*ee* (%)
10	(*R*)-3,5-Xyl-SDP(O)	96	99
11	(*S*,*S*,*S*)-SPIRAP(O)	99	-94
12	(*R*,*S*,*S*)-SPIRAP(O)	96	89

entry	ligand	yield (%)	*ee* (%)
13	(*S*)-BINAPO	84	89
14	(*S*)-SDPO	85	-93
15	(*S*,*R*,*R*)-SPIRAPO	87	-90
16	(*R*,*R*,*R*)-SPIRAPO	85	93

Scheme 4. Application of SPIRAP, SPIRAP(O), and SPIRAPO in iridium-, palladium-, and rhodium-catalyzed asymmetric transformations. A) $[IrCl(COD)]_2$ (2.5 mol %), ligand (6 mol %), $NaBAr^F_4$ (10 mol %), 2-phenylpyridine (1.07 equiv), toluene. B) $[PdCl(allyl)]_2$ (2.5 mol %), ligand (6 mol %), dimethyl malonate (2 equiv), Et_2Zn (2 equiv), RT, 1,4-dioxane. C) $Pd(dba)_2$ (2.5 mol %), ligand (3 mol %), norbornene (4 equiv), DIPEA (2 equiv), 1,4-dioxane, 70 °C. D) [Rh(COD)]OTf (5.0 mol %), ligand (6.0 mol %), H_2 (500 psi), DCM, RT.

18 with norbornene **19** to afford tricycle **20** (Scheme 4 C, entry 11).[16] As before, the diastereomeric complex (*R*,*S*,*S*)-SPIRAP(O) favored the enantiomeric product albeit with somewhat lower selectivity (entry 12). Finally, the diphosphinites (*S*,*R*,*R*)-SPIRAPO and (*R*,*R*,*R*)-SPIRAPO were applied in the rhodium-catalyzed asymmetric hydrogenation of dehydroalanine derivative **21** with excellent results.[17] (*R*,*R*,*R*)-SPIRAPO performed similarly to the SPINOL-based ligand (*S*)-SDPO (entries 16 and 14) whereas the use of the *S*,*R*,*R* diastereomer resulted in a reversal of enantio-

selectivity (entry 15). In addition, SPIROMP was used as an organocatalyst for an aza-Baylis–Hillman reaction (see the Supporting Information).[18]

The consistently similar performance of (*S*,*S*,*S*)-SPIRAP and (*S*)-SDP and the different behavior of (*R*,*S*,*S*)-SPIRAP prompted us to do a more thorough comparison of the *S*,*S*,*S* and *R*,*S*,*S* diastereomers. DFT[13,19] analysis of the diastereomeric Pd^{II} complexes of SPIRAP (**11**) and commercial (*S*)-SDP demonstrated that these complexes have similar natural charges at the metallic center. However, while the geometry index parameters τ_4[20] and τ_4'[21] showed similar values for (*S*,*S*,*S*)-**11** and (*S*)-**23** (Table 1, entries 1 and 3), τ_4 and τ_4' for

Table 1: Comparison of the three-dimensional structures of SPIRAP diastereomers and SDP.[a]

Entry	Complex	Natural charge at Pd^{II}	τ_4	τ_4'	Bite angle [°]
1	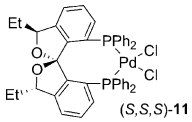 (*S*,*S*,*S*)-**11**	0.425	0.113	0.125	94.4
2	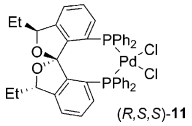 (*R*,*S*,*S*)-**11**	0.425	0.086	0.092	95.3
3	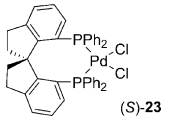 (*S*)-**23**	0.427	0.112	0.129	94.2

[a] τ_4 and τ_4' are geometry index parameters defined by the two largest angles at Pd.

(*R*,*S*,*S*)-**11** were found to be considerably different (Table 1, entry 2). This implied that although these three complexes are electronically similar, the (*R*,*S*,*S*)-SPIRAP complex is structurally significantly different from (*S*)-SDP, while (*S*,*S*,*S*)-SPIRAP, although not identical, is much more similar. The calculated bite angles also reflect this trend, with (*R*,*S*,*S*)-SPIRAP showing a slightly larger angle. This explains the lower performance of (*R*,*S*,*S*)-SPIRAP in catalytic applications optimized for SDP. A closer inspection of the three-dimensional structures of these complexes revealed that the ethyl side chain in (*R*,*S*,*S*)-SPIRAP disturbs the π-stacking between the aryl groups of the backbone, leading to a different overall geometry (Figure 2). The structural dissimilarities between our spiroketal manifold and the SPINOL core make us believe that our catalytic platform could provide a unique solution to new asymmetric methods of importance in current organic chemistry. This divergence is reflected in the performance of our ligands in some of the reactions mentioned above. The ease of preparation, the stability, the availability of new sites for tuning, and the outstanding performance of (*S*,*S*,*S*)-SPIRAP prompt us to suggest that it could be a widely used and successful ligand in asymmetric catalysis. In addition, the corresponding *R*,*S*,*S* ligands are easily accessible from the same chiral intermediate and could be used if reversed selectivity is desired. The results obtained with the *R*,*S*,*S* ligands are particularly remarkable as these ligands, which are thermodynamically less stable than the *S*,*S*,*S* diastereomers, are kinetically stable under a variety of reaction conditions. Further applications of our new ligands in novel reactions and chemical processes that will help highlight the differences between these and established SDPs, as well as the preparation of other catalysts derived from the SPIROL core, are currently underway in our laboratory.

Acknowledgements

This work was supported by the National Science Foundation (grant CHE-1350060 to P.N.). We thank Prof. Paul Zimmerman for useful discussions during the preparation of this manuscript, David Braun for computational support, and Dr. Jeff Kampf for crystallographic studies.

Conflict of interest

The authors declare no conflict of interest.

Keywords: asymmetric catalysis · iridium · palladium · phosphines · spiroketals

How to cite: *Angew. Chem. Int. Ed.* **2018**, *57*, 5325–5329
Angew. Chem. **2018**, *130*, 5423–5427

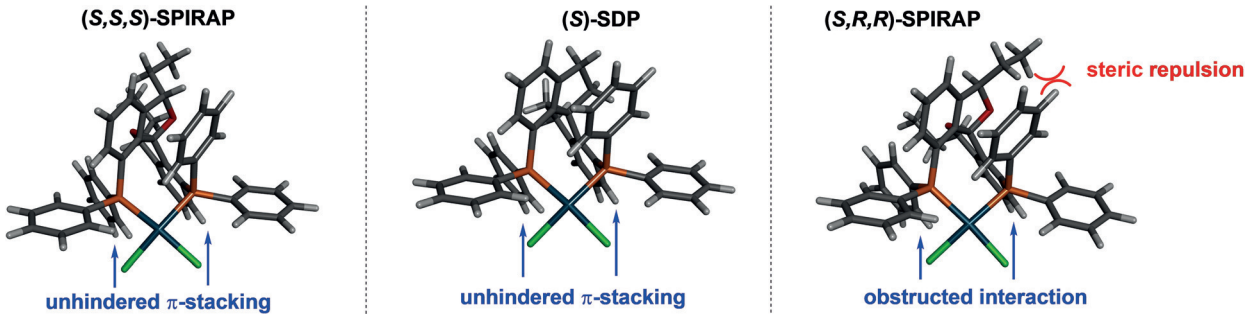

Figure 2. Comparison of (*S*,*R*,*R*)-SPIRAP, (*S*,*S*,*S*)-SPIRAP, and SDP complexes of $PdCl_2$. The geometries of (*S*,*S*,*S*)-**11**, (*R*,*S*,*S*)-**11**, and (*S*)-**25** were optimized by DFT with the B97-D exchange functional and mixed basis sets (Lanl2dz for Pd, P, and Cl and 6-31G** for all other atoms).

[1] a) S. Akutagawa, *Appl. Catal. A* **1995**, *128*, 171; b) R. Noyori, *Angew. Chem. Int. Ed.* **2002**, *41*, 2008; *Angew. Chem.* **2002**, *114*, 2108; c) C. A. Busacca, D. R. Fanrick, J. J. Song, C. H. Senanayake, *Adv. Synth. Catal.* **2011**, *353*, 1825.

[2] L. A. Adrio, K. Kuok (Mimi) Hii in *Organometallic Chemistry*, *Vol. 35* (Eds.: I. J. S. Fairlamb, J. M. Lynam), RSC Publishing, London, **2009**, pp. 62 – 92.

[3] a) T. T. L. Au-Yeung, S.-S. Chan, A. S. C. Chan, *Adv. Synth. Catal.* **2003**, *345*, 537; b) M. Berthod, G. Mignani, D. Woodward, M. Lemaire, *Chem. Rev.* **2005**, *105*, 1801; c) Q.-L. Zhou in *Privileged Chiral Ligands and Catalysts*, Wiley-VCH, Weinheim, **2011**; d) S. Lühr, J. Holz, A. Börner, *ChemCatChem* **2011**, *3*, 1708; e) M. M. Pereira, M. J. F. Calvete, R. M. B. Carrilho, A. R. Abreu, *Chem. Soc. Rev.* **2013**, *42*, 6990.

[4] For examples of chiral-phosphine-based ligand design, see: a) W. Tang, N. D. Patel, G. Xu, X. Xu, J. Savoie, S. Ma, M.-H. Hao, S. Keshipeddy, A. G. Capacci, X. Wei, Y. Zhang, J. J. Gao, W. Li, S. Rodriguez, B. Z. Lu, N. K. Yee, C. H. Senanayake, *Org. Lett.* **2012**, *14*, 2258; b) F. Maurer, V. Huch, A. Ullrich, U. Kazmaier, *J. Org. Chem.* **2012**, *77*, 5139; c) G. Liu, X. Liu, Z. Cai, G. Jiao, G. Xu, W. Tang, *Angew. Chem. Int. Ed.* **2013**, *52*, 4235; *Angew. Chem.* **2013**, *125*, 4329; d) F. S. P. Cardoso, K. A. Abboud, A. Aponick, *J. Am. Chem. Soc.* **2013**, *135*, 14548; e) J. Graff, E. Lastawiecka, L. Guenee, F. Leroux, A. Alexakis, *Adv. Synth. Catal.* **2015**, *357*, 2833; f) P. Ramírez-López, A. Ros, B. Estepa, R. Fernández, B. Fiser, E. Gómez-Bengoa, J. M. Lassaletta, *ACS Catal.* **2016**, *6*, 3955; g) S. Mishra, A. Aponick, *J. Am. Chem. Soc.* **2017**, *139*, 3352; h) P. H. S. Paioti, K. A. Abboud, A. Aponick, *ACS Catal.* **2017**, *7*, 2133; i) F. Sartorius, M. Trebing, C. Brückner, R. Brückner, *Chem. Eur. J.* **2017**, *23*, 17463.

[5] a) V. B. Birman, A. L. Rheingold, K.-C. Lam, *Tetrahedron: Asymmetry* **1999**, *10*, 125; b) J.-H. Zhang, J. Liao, X. Cui, K.-B. Yu, J.-G. Deng, S.-F. Zhu, L.-X. Wang, Q.-L. Zhou, L. W. Chung, T. Ye, *Tetrahedron: Asymmetry* **2002**, *13*, 1363; c) J. H. Xie, L. X. Wang, Y. Fu, S. F. Zhu, B. M. Fan, H. F. Duan, Q.-L. Zhou, *J. Am. Chem. Soc.* **2003**, *125*, 4404.

[6] For selected reviews, see: a) J. H. Xie, Q.-L. Zhou, *Acc. Chem. Res.* **2008**, *41*, 581; b) K. Ding, Z. Han, Z. Wang, *Chem. Asian J.* **2009**, *4*, 32.

[7] S. Li, J.-W. Zhang, X.-L. Li, D.-J. Cheng, B. Tan, *J. Am. Chem. Soc.* **2016**, *138*, 16561.

[8] a) Z. Sun, G. A. Winschel, A. Borovika, P. Nagorny, *J. Am. Chem. Soc.* **2012**, *134*, 8074; b) P. Nagorny, Z. Sun, G. A. Winschel, *Synlett* **2013**, 661; c) Y. Y. Khomutnyk, A. J. Argüelles, G. A. Winschel, Z. Sun, P. M. Zimmerman, *J. Am. Chem. Soc.* **2016**, *138*, 444.

[9] a) T. P. Dang, H. B. Kagan, *J. Chem. Soc.* **1971**, *10*, 481; b) H. Shimizu, I. Nagasaki, K. Matsumura, N. Sayo, T. Saito, *Acc. Chem. Res.* **2007**, *40*, 1385; c) C. M. Lavoie, P. M. MacQueen, N. L. Rotta-Loria, R. S. Sawatzky, A. Borzenko, A. J. Chisholm, B. K. V. Hargreaves, R. McDonald, R. M. J. Ferguson, M. Stradiotto, *Nat. Commun.* **2016**, *7*, 11073.

[10] a) X. Wang, Z. Han, Z. Wang, K. Ding, *Angew. Chem. Int. Ed.* **2012**, *51*, 936; *Angew. Chem.* **2012**, *124*, 960; b) Z.-Y. Cao, X. Wang, C. Tan, X.-L. Zhao, J. Zhou, K. Ding, *J. Am. Chem. Soc.* **2013**, *135*, 8197.

[11] K. Soai, S. Yokoyama, T. Hayasaka, *J. Org. Chem.* **1991**, *56*, 4264.

[12] M.-C. Wang, Y.-H. Wang, G.-W. Li, P.-P. Sun, J.-X. Tian, H.-J. Lu, *Tetrahedron: Asymmetry* **2011**, *22*, 761.

[13] Computations were carried out using the Q-Chem. quantum-chemical package at the ωB97x-D level of theory with a mixed basis set (6-31G** and lanl2dz). Natural bond orbital (NBO) analysis was carried out using NBO 5.0. Additional details and full citations are included in the Supporting Information.

[14] Y. Ebe, M. Onoda, T. Nishimura, H. Yorimitsu, *Angew. Chem. Int. Ed.* **2017**, *56*, 5607; *Angew. Chem.* **2017**, *129*, 5699.

[15] J. H. Xie, H. F. Duan, B. M. Fan, X. Cheng, L. X. Wang, Q.-L. Zhou, *Adv. Synth. Catal.* **2004**, *346*, 625.

[16] J. Hu, H. Hirao, Y. Li, J. S. Zhou, *Angew. Chem. Int. Ed.* **2013**, *52*, 8676; *Angew. Chem.* **2013**, *125*, 8838.

[17] R. Guo, T. T.-L. Au-Yeung, J. Wu, M. C. K. Choi, A. S. C. Chan, *Tetrahedron: Asymmetry* **2002**, *13*, 2519.

[18] S. Takizawa, K. Kiriyama, K. Ieki, H. Sasai, *Chem. Commun.* **2011**, *47*, 9227.

[19] P. Geerlings, F. De Proft, W. Langenaeker, *Chem. Rev.* **2003**, *103*, 1793.

[20] L. Yang, D. R. Powell, R. P. Houser, *Dalton Trans.* **2007**, 955.

[21] A. Okuniewski, D. Rosiak, J. Chojnacki, B. Becker, *Polyhedron* **2015**, *90*, 47.

Manuscript received: December 26, 2017
Revised manuscript received: February 6, 2018
Accepted manuscript online: February 22, 2018
Version of record online: March 23, 2018

